Experimental Simulation of Two-Particle Quantum Entanglement using Classical Fields

K. F. Lee and J. E. Thomas

Physics Department, Duke University, Durham, North Carolina 27708-0305
(Received 25 June 2001; revised manuscript received 13 November 2001; published 12 February 2002)

We experimentally demonstrate simulation of two entangled quantum bits using classical fields of two frequencies and two polarizations. Multiplication of optical heterodyne beat signals from two spatially separated regions simulates coincidence detection of two particles. The product signal so obtained contains several frequency components, one of which can be selected by bandpass frequency filtering. The bandpassed signal contains two indistinguishable, interfering contributions, permitting simulation of four polarization-entangled Bell-like states. These classical field methods may be useful in small scale simulations of quantum logic operations that require multiparticle entanglement without collapse.

Currently, there is great interest in classical-wave simulation of quantum logic [1–3] and quantum measurement [4]. Classical-wave simulation is equivalent to an analog electronic computer which reproduces the interferences that arise in a quantum system [3]. Analogous to quantum systems, classical-wave fields obey a superposition principle, enabling operations with superposition states on which much of the quantum information processing is based. Since decoherence is readily avoided, classical fields are well suited for simulating the unitary evolution of a quantum system. In addition to potential practical applications, study of classical-wave systems will help to elucidate the fundamental differences between classical-wave and quantum systems. Although it has been pointed out by several authors that classical-wave simulation of n single particle quantum bits (qubits) should exhibit exponential scaling of the number of optical paths with n, the ability to perform unitary operations with simple beam splitters and polarizers [1] makes classical-wave analogs useful for simulating small-scale quantum systems.

An important feature often associated with quantum systems is the concept of entanglement which describes correlations between different degrees of freedom. Two types of entanglement have been identified [1–3]: (i) nonlocal entanglement between separate particles and (ii) local entanglement between different properties of a single particle, such as polarization and momentum. It has been shown theoretically that classical-wave systems which simulate type (ii) quantum entanglement fail to simulate quantum nonlocality because a single particle cannot be sent to two spatially separated observers. Classical simulation of type (ii) entanglement has been discussed in detail, including quantum information processing and violation of generalized Bell's inequalities which depend only on sums of single particle detection signals [3]. It has also been shown that single photon quantum interference can be fully simulated by classical-wave interference [5]. Recently, a hybrid approach has been suggested to implement type (i) entanglement using quantum nondemolition measurement to entangle separated one-photon interferometers [6]. While a variety of classical-wave schemes for simu-

lating quantum logic have been proposed, relatively few have been implemented. Further, the proposed schemes have been limited to single-particle entanglement.

In this Letter, we describe and demonstrate a simple, general method for classical-wave simulation of type (i) entanglement of more than one particle. The simulations employ optical heterodyne detection of fields of different frequencies. The field at each frequency is a classical analog (c-bit) of a qubit which can be in an arbitrary polarization state, i.e., a superposition of two orthogonal polarizations. Essential to the method is the use of analog multiplication of the heterodyne signals from independent spatially separated detectors to simulate coincidence measurement of multiple particles. The product signal so obtained contains several frequency components, one of which can be selected by bandpass frequency filtering. The bandpassed signal generally contains several indistinguishable, interfering contributions, permitting simulation of a specific multiparticle entangled state.

Our experiments simulate entanglement of two c-bits. The first is a beam of frequency $\omega_V = \omega + 2\pi \times 100$ kHz with vertical polarization which is combined on a 50-50 beam splitter with a second c-bit which is a beam of frequency $\omega_H = \omega + 2\pi \times 25$ kHz with horizontal polarization. In the "parenthesis" notation of Ref. [3], the two output fields of the beam splitter can be represented as states $|\psi_1\rangle = [|H1\rangle \exp(-i\omega_H t) + |V1\rangle \exp(-i\omega_V t)]/\sqrt{2}$ and $|\psi_2\rangle = [|H2\rangle \exp(-i\omega_H t) - |V2\rangle \exp(-i\omega_V t)]/\sqrt{2}$. These output beams are sent to two spatially separated measurement systems, each of which employs heterodyne detection with an independent local oscillator (LO) of frequency ω and a variable polarization θ_1 and θ_2, respectively. For arbitrary polarizations, each heterodyne signal contains two frequency components, at 25 and 100 kHz. These signals are multiplied together in an analog multiplier, and the product signal is bandpassed at 125 kHz to obtain a signal containing two indistinguishable contributions, one from $|V1\rangle|H2\rangle$ which is $\propto \cos\theta_1 \sin\theta_2$ and one from $-|H1\rangle|V2\rangle$ which is $\propto -\sin\theta_1 \cos\theta_2$. The squared magnitude of the product signal at 125 kHz is then $\propto \sin^2(\theta_1 - \theta_2)$, independent of the phases of the

independent LO fields. The angle dependence is identical to the joint probability obtained in quantum mechanical experiments employing coincidence counting of correlated, orthogonally polarized, signal and idler photon pairs generated by parametric down-conversion [7]. Since a single classical beam can contain fields of many frequencies each of arbitrary polarization, this method is readily generalized to explore entanglement of more than two particles.

Previously, classical-wave analogs of the Schrödinger wave function have been explored both theoretically and experimentally. It is well known that, in the paraxial approximation, the transverse mode of an electromagnetic field obeys a propagation equation which is formally identical to the Schrödinger equation with the time replaced by the axial coordinate. Hence, the transverse modes of the field in a lenslike medium are identical in structure to harmonic oscillator wave functions in two dimensions [8]. This has led to the study of a number of classical-wave analogs of quantum wave mechanics, including analogs of Fock states [9,10] and measurement of Wigner phase-space distributions for classical optical fields which can exhibit negative regions [11–14]. However, exploration of classical analogs has been limited principally to measurement of first order coherence, i.e., single-particle states. Classical-wave analogs of higher order coherence, i.e., multiparticle states, have been relatively unexplored.

In our experiments (Fig. 1), a HeNe laser beam is split and sent through two fixed-frequency acousto-optic modulators to produce a beam of frequency $\omega_H = \omega + \delta_{horiz}$ with horizontal polarization and a beam of frequency $\omega_V = \omega + \delta_{vert}$ with vertical polarization, where $\delta_{horiz} = 2\pi \times 25$ kHz and $\delta_{vert} = 2\pi \times 100$ kHz. These two beams are combined on beam splitter BS1. Note that the relative phase between the 25 and 100 kHz fields is the same for each port of BS1, except for a π phase shift which arises from the beam splitter. The total output field from each port 1 and 2, denoted $\mathbf{E}_1$ and $\mathbf{E}_2$, is sent to heterodyne detection systems at beam splitters BS2 and BS3, respectively. Here, they are mixed with independent local oscillator beams LO1 and LO2 of variable polarizations and equal frequencies ω. The LO polarizations are controlled by independent half-wave plates, and are given by

$$\hat{\mathbf{e}}_{LO1} = \cos\theta_1 \hat{V} + \sin\theta_1 \hat{H}$$
$$\hat{\mathbf{e}}_{LO2} = \cos\theta_2 \hat{V} + \sin\theta_2 \hat{H}, \tag{1}$$

where H (V) denotes the horizontal (vertical) direction. The beat signal amplitudes A_1 and A_2, at the outputs of BS2 and BS3, respectively, can be represented as inner products in the parenthesis notation of Ref. [3],

$$A_1 = (E_{LO1}|1)$$
$$\equiv \int dx\, dy\, E_{LO1}^*(x,y,t)\hat{\mathbf{e}}_{LO1}^* \cdot \mathbf{E}_1(x,y,t), \tag{2}$$

and similarly for LO2. Here, $E_{LO1}(x,y,t) = \mathcal{E}_{LO1}(x,y) \times \exp(-i\omega t)$ is the LO1 field in the plane of a photodiode

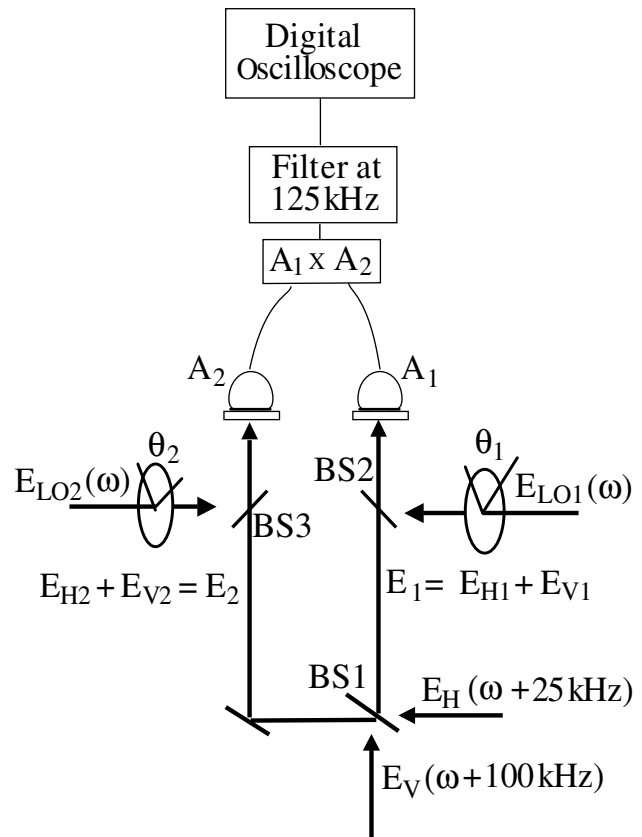FIG. 1. Experimental arrangement. Local oscillators at frequency ω and linear polarizations θ_1 and θ_2 are mixed with fields E_1 and E_2, respectively. The detected beat signals are multiplied together and band pass filtered at 125 kHz, yielding a product signal containing two indistinguishable contributions in the horizontal-vertical product basis. The squared magnitude of the product signal at 125 kHz is determined as a function of θ_1 and θ_2 to simulate coincidence measurement of two particles.

detector and $\mathbf{E}_1$ is the vector field amplitude from port 1 of BS1. The beat signals are sent to an analog multiplier which yields a product signal proportional to the real part of the amplitude $A_1 A_2 + A_1^* A_2$.

To select a particular classically entangled state, we take advantage of the fact that the product signal contains four different frequencies: The fields $\mathbf{E}_1$ and $\mathbf{E}_2$ contain frequencies $\omega + \delta_{horiz}$ and $\omega + \delta_{vert}$. Hence, for arbitrary LO polarizations, the beat amplitudes A_1 and A_2 each contain two beat frequencies δ_{horiz} and δ_{vert}, yielding four nonzero frequency components in the product signal: $\delta_{horiz} \pm \delta_{vert}$, $2\delta_{horiz}$ and $2\delta_{vert}$. A bandpass filter is used to select the product signal at frequency $\Delta_+ \equiv \delta_{horiz} + \delta_{vert} = 125$ kHz. In this case, we measure only the signal corresponding to the real part of the amplitude $A_1 A_2$ which contains two contributions:

$$\gamma(\theta_1, \theta_2) \propto \sin\theta_1 \cos\theta_2 (\mathcal{E}_{LO1}|\mathcal{E}_{H1})(\mathcal{E}_{LO2}|\mathcal{E}_{V2})$$
$$\pm \cos\theta_1 \sin\theta_2 (\mathcal{E}_{LO1}|\mathcal{E}_{V1})(\mathcal{E}_{LO2}|\mathcal{E}_{H2}). \tag{3}$$

Here, $(\mathcal{E}_{LO1}|\mathcal{E}_{H1})$ denotes the spatial overlap integral of LO1 and the horizontal component of the field from port 1

of BS1, and similarly for the other overlap integrals. The relative sign $\pm$ is controlled by placing a half-wave plate oriented at a zero degree angle in one output of BS1. The two terms in Eq. (3) arise because there are two ways to obtain a product signal at frequency 125 kHz. Note that the products of the spatial overlap integrals have the same amplitude and phase in both terms, i.e., $(\mathcal{E}_{LO1}|\mathcal{E}_{H1}) \times (\mathcal{E}_{LO2}|\mathcal{E}_{V2}) = (\mathcal{E}_{LO1}|\mathcal{E}_{V1})(\mathcal{E}_{LO2}|\mathcal{E}_{H2})$, which factors out in the signal amplitude. Hence, the overall phases of LO1 and LO2 cancel in the measurements, and the signal can be normalized by finding the maximum value with $\theta_1 = 45° = \pm\theta_2$. Dividing by the maximum value yields the normalized signal amplitude $\gamma_N(\theta_1, \theta_2) = \sin(\theta_1 \pm \theta_2)$.

The signal amplitude at 125 kHz can be rewritten in the form $\gamma(\theta_1, \theta_2) \propto (\hat{e}_{LO1}, \hat{e}_{LO2}|\Psi_{\pm}^{cl})_{\Delta_+}$ where $|\Psi_{\pm}^{cl})_{\Delta_+}$ are the classical analogs of the entangled states

$$|\Psi_{\pm}^{cl})_{\Delta_+} \equiv \frac{1}{\sqrt{2}}[|H1)|V2) \pm |V1)|H2)]. \quad (4)$$

Here, $|H1)$ arises from the 25 kHz horizontally polarized field from port 1, etc. Equation (4) shows that classical analogs of two different Bell states can be measured. The other two Bell states can be obtained by inserting a half-wave plate oriented at 45° in one output of BS1. This interchanges the horizontal and vertical frequencies in one port so that the product signal at frequency Δ_+ contains the polarization states $|H_1)|H_2)$ and $|V_1)|V_2)$,

$$|\varphi_{\pm}^{cl})_{\Delta_+} \equiv \frac{1}{\sqrt{2}}[|H1)|H2) \pm |V1)|V2)]. \quad (5)$$

Here, the relative sign is again controlled by using an additional half-wave plate oriented along the output V axis of one port.

By measuring the magnitude of $\gamma(\theta_1, \theta_2)$ using a digital oscilloscope (or lock-in detection at the frequency Δ_+), we obtain $|\gamma_N(\theta_1, \theta_2)|^2$. Hence, after normalization to the maximum signal, we measure the classical joint intensity $P_{cl}(\hat{e}_{LO1}, \hat{e}_{LO2}) = |\gamma_N(\theta_1, \theta_2)|^2 = \sin^2(\theta_1 \pm \theta_2)$.

Note that, if Eq. (4) were a true, normalized quantum state, then the joint probability for coincidence detection of two photons with polarizations $\hat{e}(\theta_1)$ and $\hat{e}(\theta_2)$ would be $\sin^2(\theta_1 \pm \theta_2)/2$. This differs from our classical result only by a multiplicative factor of $1/2$, arising from our choice of normalization.

In Fig. 2(a), we measure the quantity $|\gamma_N(\theta_1 = 30°, \theta_2)|^2$ for the state $|\Psi^{cl})$ of Eq. (4) as a function of θ_2 between $-90°$ and $90°$. The solid line is the theoretical prediction with $|\gamma_N(\theta_1, \theta_2)|^2 = \sin^2(\theta_1 - \theta_2)$. By inserting a half-wave plate in one port, we have measured $|\gamma_N|^2$ for the state $|\Psi_+^{cl})$, where $|\gamma_N(\theta_1, \theta_2)|^2 = \sin^2(\theta_1 + \theta_2)$ (not shown).

To measure the other two Bell states, $|\varphi_{\pm}^{cl})$, of Eq. (5), we insert a half-wave plate oriented at 45° in one output of BS1. A second half-wave plate oriented at 0° selects the relative phase $\pm$. In this case, $|\gamma_N(\theta_1, \theta_2)|^2 =$
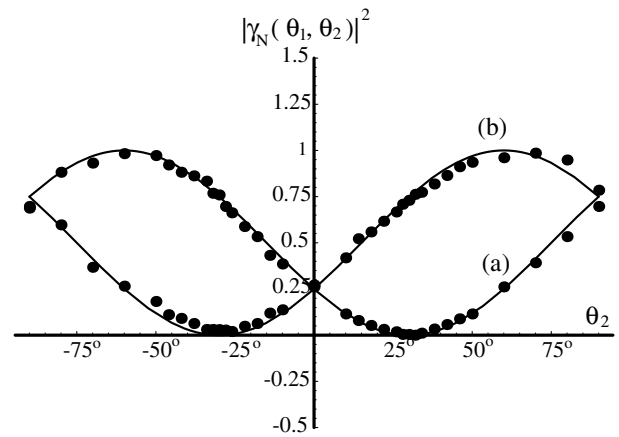

FIG. 2.   Measured joint intensity $|\gamma_N(\theta_1, \theta_2)|^2$ as a function of θ_2 for the Bell states: (a) $(1/\sqrt{2})[|H_1)|V_2) - |V_1)|H_2)]$ with $\theta_1 = 30°$ and (b) $(1/\sqrt{2})[|H_1)|H_2) + |V_1)|V_2)]$ with $\theta_1 = 60°$.

$\cos^2(\theta_1 \mp \theta_2)$. Normalization is accomplished by measuring the maximum product signal with $\theta_1 = 45°$ and $\theta_2 = \pm 45°$. For the $|\varphi_+^{cl})$ state, measurements of the quantity $|\gamma_N(60°, \theta_2)|^2$ are shown in Fig. 2(b). We have also measured $|\gamma_N(60°, \theta_2)|^2$ for the state $|\varphi_-^{cl})$ (not shown).

For each of the four Bell states, the measured joint intensities take the same form as in a quantum joint-probability measurement. Hence, it is possible to violate formally a classical analog of the Bell inequality used in recent quantum measurements of the joint detection probability for entangled photon pairs [15,16]:

$$F_{cl}(\mathbf{a}, \mathbf{b}, \mathbf{c}) \equiv P_{cl}(\mathbf{a}, \mathbf{b}) + P_{cl}(\mathbf{b}, \mathbf{c}) - P_{cl}(\mathbf{a}, \mathbf{c}) \geq 0, \quad (6)$$

where $P_{cl}(\mathbf{a}, \mathbf{b}) = |\gamma_N(\theta_a, \theta_b)|^2$ is the joint intensity when the local oscillators have linear polarizations $\mathbf{a}$ and $\mathbf{b}$, respectively.

By proper choice of angles for the polarizations $\mathbf{a}, \mathbf{b}, \mathbf{c}$ in Eq. (6), the classical joint intensity exhibits a maximum violation of the Bell inequality $F_{cl} \geq 0$. To demonstrate the violation for the state $|\Psi_+^{cl})$ of Eq. (4), we take $\mathbf{b} = \hat{V}$, i.e., $\theta_B = 0°$, $\mathbf{a} = \mathbf{c}$ and measure $F_{cl}(\mathbf{a}, \mathbf{b}, \mathbf{c})$ of Eq. (6) as a function of $\theta_a = \theta_c = \theta$ for θ between $0°$ and $90°$. We obtain the data shown in Fig. 3. The maximum violation occurs at $\theta = 30°$, as in a quantum joint probability measurement, and has the value $F_{cl} = -0.25$. The solid line shows the prediction $F_{cl}(\theta, 0°, \theta) = |\gamma_N(\theta, 0°)|^2 + |\gamma_N(0°, \theta)|^2 - |\gamma_N(\theta, \theta)|^2$, where $|\gamma_N(\theta_1, \theta_2)|^2 = \sin^2(\theta_1 + \theta_2)$.

The results of the frequency selected measurements are identical in structure with the predictions of analogous quantum optics experiments. The correlated polarization measurements for our polarization-entangled Bell states demonstrate a violation of Bell's inequality very similar to that obtained using polarization-entangled photons from a parametric down-converter, where coincidence detection performed a postprojection of the entangled state [7]. Further, the joint intensities depend only on $\theta_1 \pm \theta_2$, so that
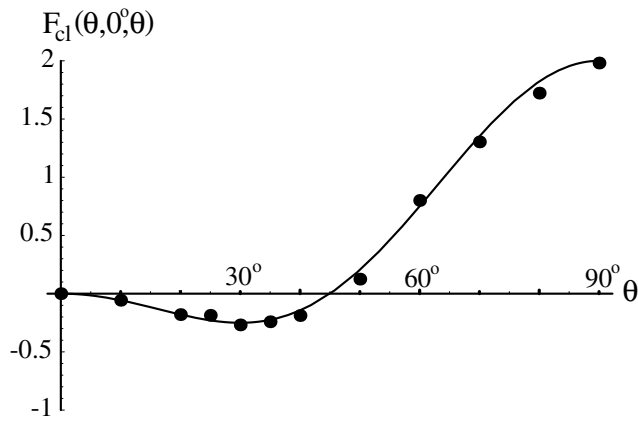
$F_{cl}(\theta, 0, \theta)$

FIG. 3. Classical simulation of Bell's inequality violation for the $|\Psi_+^{cl}\rangle$ state. A classical analog of the inequality is $F_{cl}(\theta, 0, \theta) \geq 0$. The maximum violation, $F_{cl}(\theta, 0, \theta) = -0.25$, occurs when $\theta = 30°$.

the results do not depend on a particular orientation of either LO. However, the system does not exhibit particle-like behavior or collapse, so that Bell's inequalities are not strictly applicable. Hence, if our experiments were done using polarizing beam splitters in the two detection regions (and LO's with 45° polarization), all outputs would contain signals simultaneously. By contrast, in a true two-photon experiment, if a photon is detected in the horizontal port for beam 1, the polarization of the photon detected in beam 2 must be vertical. In our classical simulation, this corresponds to setting the LO in port 1 to project out the horizontal component, so that the signal from detector 1 is at 25 kHz. If the product of this signal and that obtained at port 2 is obtained and bandpass filtered at 125 kHz as before, then the maximum signal is obtained when the LO in port 2 is vertically polarized. Of course, our scheme does not prepare a true entangled state, but we measure a classical analog by postprojection using the appropriate frequency.

In conclusion, we have shown that analog multiplication of heterodyne signals arising from classical fields leads to measurement in a product basis and permits simulation of multiparticle entanglement. Our method of signal multiplication and frequency selection enables straightforward simulation of higher order interference for a variety of quantum experiments which employ linear optical systems. For example, we have simulated a four-particle entangled state, such as $|\Psi\rangle \propto |H_1\rangle |H_2\rangle |H_3\rangle |H_4\rangle + |V_1\rangle |V_2\rangle |V_3\rangle |V_4\rangle$. The experiments use two beam splitters and four beam heterodyne detection, followed by analog multiplication of the four signals and appropriate sum frequency selection. Using this method, we have been able to reproduce the truth tables of a recent Greenberger-Horne-Zeilinger experiment [17] by using an optical system nearly identical to the quantum version, but replacing the source by a combination of fields of two frequencies. It is also possible to reproduce the behavior of two-photon interferometers for which the fringe frequency is twice that of a one-photon interferometer. In view of the stability and high signal-to-noise ratio obtainable using classical optical waves and the potential for producing observations analogous to those of a quantum system, the study of classical-wave analogs of quantum optics appears to be a worthwhile goal. Exploration of classical-wave analogs may yield new insights into quantum communication, quantum cryptography, and error correction schemes. In addition, such studies may provide useful insights into fundamental features of quantum mechanics.

[1] N. J. Cerf, C. Adami, and P. G. Kwiat, Phys. Rev. A **57**, R1477 (1998).
[2] R. J. C. Spreeuw, Phys. Rev. A **63**, 062302 (2001).
[3] R. J. C. Spreeuw, Found. Phys. **28**, 361 (1998).
[4] S. Massar, D. Bacon, N. J. Cerf, and R. Cleve, Phys. Rev. A **63**, 052305 (2001).
[5] S. Wallentowitz, I. A. Walmsley, and J. H. Eberly, quant-ph/0009069, 2000.
[6] J. C. Howell and J. A. Yeazell, Phys. Rev. Lett. **85**, 198 (2000).
[7] Z. Y. Ou and L. Mandel, Phys. Rev. Lett. **61**, 50 (1988).
[8] A. Yariv, *Introduction to Optical Electronics* (Holt, Rinehart and Winston, New York, 1976), Chap. 3.
[9] D. Dragoman, Optik (Stuttgart) **111**, 393 (2000).
[10] K. Wódkiewicz and G. H. Herling, Phys. Rev. A **57**, 815 (1998).
[11] C. Iaconis and I. A. Walmsley, Opt. Lett. **21**, 1783 (1996).
[12] C.-C. Cheng and M. G. Raymer, Phys. Rev. Lett. **82**, 4807 (1999).
[13] K. F. Lee, F. Reil, S. Bali, A. Wax, and J. E. Thomas, Opt. Lett. **24**, 1370 (1999).
[14] D. Dragoman, Optik (Stuttgart) **111**, 179 (2000).
[15] T. Jennewein, C. Simon, G. Weihs, H. Weinfurter, and A. Zeilinger, Phys. Rev. Lett. **84**, 4729 (2000).
[16] E. P. Wigner, Am. J. Phys. **38**, 1005 (1970).
[17] J.-W. Pan, D. Bouwmeester, M. Daniell, H. Weinfurter, and A. Zeilinger, Nature (London) **403**, 515 (2000).